International Journal of Applied and Natural Sciences (IJANS)
ISSN(P): 2319-4014; ISSN(E): 2319-4022
Vol. 3, Issue 2, Mar 2014, 63-80

International Academy of Science, Engineering and Technology
Connecting Researchers; Nurturing Innovations

INVESTIGATION ON *N*-FORMYL PIPERIDIN-4-ONES AS CORROSION INHIBITORS FOR CARBON STEEL IN ACID MEDIUM

A. ILAMPARITHI[1], S. PONNUSWAMY[2] & A. SELVARAJ[3]

[1,2]PG and Research, Department of Chemistry, Government Arts College (Autonomous), Coimbatore, Tamil Nadu, India

[1]Department of Chemistry, Gobi Arts and Science College, Gobichettipalayam, Tamil Nadu, India

[3]PG and Research, Department of Chemistry, CBM College, Coimbatore, Tamil Nadu, India

ABSTRACT

The corrosion inhibition of mild steel in 1N H_2SO_4 and 1N HCl in the presence of *N*-formyl piperidin-4-ones was studied using gravimetric and electrochemical techniques. Results obtained show that these compounds are excellent inhibitors and inhibit better in HCl than in H_2SO_4. The potentiodynamic polarisation studies clearly reveal that they are mixed type inhibitors. The impedance parameters (R_{ct} and C_{dl}) clearly indicate the adsorption of *N*-formyl piperidin-4-ones on the metal surface leading to the formation of a protective layer which grows with increasing exposure time. The adsorption of *N*-formyl derivatives on mild steel surface in both the acid media follows a Langmuir adsorption isotherm and Tempkin adsorption isotherm. The mild steel-FP complex layer formed at the metal surface was identified by infrared spectral analysis and SEM/EDS.

KEYWORDS: 1. Corrosion Inhibitors, 2. Mild Steel, 3. Electrochemical Impedance Spectroscopy, 4. Polarisation Curves, 5. Adsorption Isotherm, 6. *N*-Formyl Piperidin-4-One, 7. FT-IR , 8. SEM/EDS

INTRODUCTION

Generally HCl and H_2SO_4 are employed in the treatment of steel and ferrous alloys in industry. The use of inhibitors containing heteroatom's like nitrogen, oxygen, and sulphur is one of the most practical methods for protection against corrosion in acid media [1]. The aim of this study is to investigate the inhibitive properties of some azacyclic inhibitors *viz.* *N*-formyl-*t*-3-methyl-*r*-2,*c*-6-diphenylpiperidin-4-one (F3MPO), *N*-formyl-*t*-3-isopropyl-*r*-2, *c*-6-diphenylpiperidin-4-one (F3IPPO), *N*-formyl *c-3,t*-3-dimethyl-*r*-2,*c*-6-diphenylpiperidin-4-one (F3DMPO) and *N*-formyl *t*-3,*c*-5-dimethyl-*r*-2,*c*-6-diphenylpiperidin-4-one (FDMPO) on the corrosion of mild steel in sulphuric acid and hydrochloric acid. The chemical structures of the inhibitors are given in Figure 1.

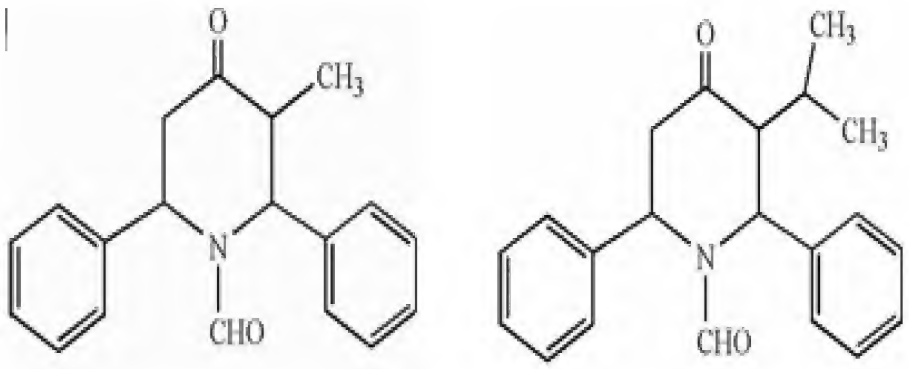

(A) **(B)**

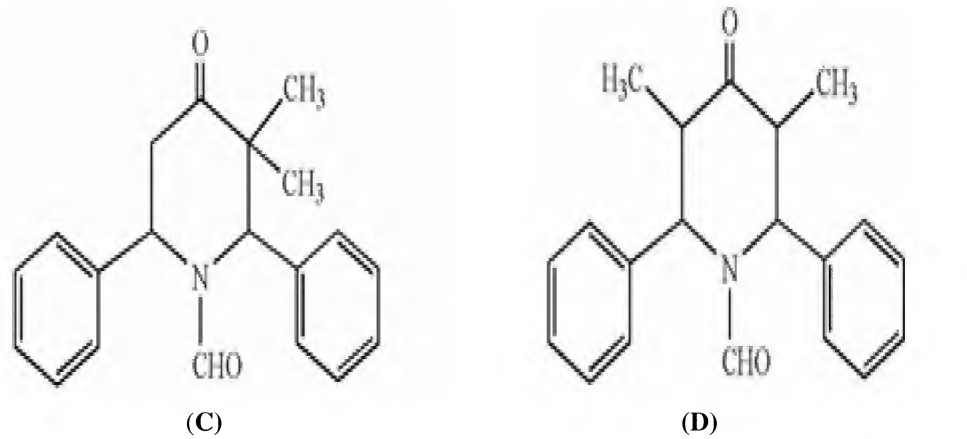

(C) (D)

Figure 1: Structure of Inhibitors (A) F3MPO (B) F3IPPO (C) F3DMPO (D) FDMPO

EXPERIMENTAL

Weight Loss Measurements

Mild steel specimens containing 0.0224% C, 0.025% Si, 0.320% Mn, 0.023% P, 0.052% S, 0.108% Ni, 0.069% Cr, 0.012% Mo, 0.047% Al, 0.011% Cu the remainder being Fe of the dimension 2.5cm×1cm×0.1cm were polished to a mirror finish using 200, 400, 600, and 800 grade emery papers and degreased with trichloroethylene and used for weight loss measurements. *N*-formyl piperidin-4-ones were synthesized as reported in literature [2-10]. Three mild steel strips were immersed in 100 ml of inhibited and uninhibited solution of 1N HCl and 1N H_2SO_4 for 3 h and their inhibition efficiency were determined. The efficiency was also studied at various elevated temperatures up to 323K and the weight loss measurements were also made at various time of immersion up to 24h. The corrosion rate (mm/Y), surface coverage [θ] and inhibition efficiency were calculated from the difference in weight loss values. Since the solubility of inhibitor is less and in order to avoid precipitation, 40 ml ethyl alcohol was added, to make up the solution, for all gravimetric and electrochemical studies.

Electrochemical Analysis

For electrochemical measurements, the cell used was a conventional three-electrode Pyrex glass cell with a platinum counter electrode and a saturated calomel electrode (SCE) as reference. The working steel rod electrode was embedded in Teflon so that it's cross sectional area (1 cm^2) was in contact with the solution. The potentiodynamic current – potential curves were recorded by changing the electrode potential automatically from -200 to +200 mV with respect to OCP and at the scan rate of 1mV s^{-1}. Electrochemical impedance spectra (EIS) were carried out at E_{corr} by using a Potentiostat/ Galvanostat/ FRA2 (μ Autolab type 3). Data were collected and analysed by Ivium software. The EIS data were acquired in the frequency range of 100 kHz to 1Hz with a 10 mV amplitude sine wave generated by a frequency response analyzer.

RESULTS AND DISCUSSIONS

Weight Loss Measurements

Table 1 gives the values of the inhibition efficiency obtained from the weight loss measurements of mild steel for different concentration of F3MPO, F3IPPO, F3DMPO and FDMPO in 1N HCl and 1N H_2SO_4 at 30^o C after 3 h immersion. F3MPO, F3IPPO, F3DMPO and FDMPO inhibit the corrosion of mild steel in an identical manner. In both the media, the inhibition efficiency increases with the increasing inhibitor concentration in the experimental condition.

The inhibition is estimated to be superior in HCl than in H_2SO_4 [11] and the optimum concentration required to achieve maximum efficiency was found to be 5 mM. F3IPPO is the best inhibitor and the efficiency decreases in the order F3IPPO>F3MPO>F3DMPO>FDMPO, in both the media. The same order was proposed by Sankarapapavinasam *et al.*[12] for the change of alkyl substituents of the parent piperidine-4-ones. It is apparent that the inhibition efficiency increases with increase in inhibitor concentration. It may be due to the fact that the extent of adsorption increases with the increase in concentration of the inhibitor leading to increased inhibition efficiency [13]. Perusal of Table 2 indicates that the IE(%) increases with the increase in immersion time from 1 to 12 h and remains constant thereafter. The available active sites on the metal surface seem to be covered by the inhibitor molecules completely in 12 h and thereafter rate of adsorption and desorption is same and hence the inhibiting efficiency remains constant [14].

Effect of Addition of 1 mM Anions on the Corrosion Inhibition of MS in H_2SO_4

In order to understand the synergistic and antagonistic effect of anions on the corrosion inhibition efficiency of the inhibitors, the following 1 mM anions *viz.* KCl, KBr, KI, KNO_3, $KBrO_3$, and KCNS were added and their efficiency was determined and shown in Table 3. The NO_3^- ion and CNS^- ion have poor synergetic effect and the synergistic effect increases in the order $Cl^-<Br^-<I^-$ as reported in the literature [15].

Effect of halide ions on the enhancing corrosion inhibition has also been studied by Hackermann *et al.* [16] who suggested that halide ions in general and especially iodide ion affect the steel dissolution by strong chemisorption on the metal surface and renders the surface more negatively charged. On the highly negatively charged metal surface the protonated cationic inhibitor molecules are adsorbed due to the electrostatic interaction. The interaction will be higher for I^- than for Cl^- or Br^- due to higher magnitude of negative charge on the metal surface. Hence the observed order is $Cl^-<Br^-<I^-$.

Effect of Temperature

To calculate the thermodynamic parameters (E_a, $\Delta H^{\#}$ and $\Delta S^{\#}$) of the corrosion process and to investigate the mechanism of the inhibition process, the weight loss measurements were recorded at various temperatures (303 K to 323 K). The data obtained for the effect of temperature on the corrosion inhibition of mild steel in 1N H_2SO_4 in presence and absence of various inhibitors are presented in Table 4. It has been found that the weight loss and the IE (%) have increased linearly with the increase of temperature in the absence and presence of inhibitors upto 323 K.

The data obtained from weight loss measurements were plotted in accordance to Arrhenius Equation and shown in Figure 2.

$$\ln \text{rate} = (-E_a / RT) + \text{Constant} \quad (1)$$

Where E_a = activation energy; R = gas constant and T= absolute temperature. The activation energies for the corrosion process are estimated from the slopes of the lines of the Arrhenius plot and given in Table 5. The values of E_a for the inhibited systems were slightly lower than those of the uninhibited system.

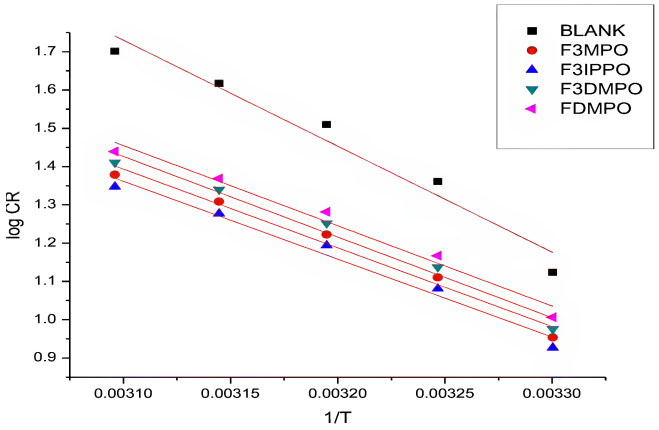

Figure 2: The Arrhenius Plots of MS Corrosion in 1N H_2SO_4 Solution Containing Inhibitors

The thermodynamic functions viz standard free energy of adsorption ΔG^o, enthalpy of adsorption $\Delta H^\#$ and entropy of adsorption $\Delta S^\#$ are estimated from the transition state plot (Figure 3) and the results are given in Table 5, 6. The negative value of ΔG^o indicates strong interaction of inhibitor molecule and spontaneous adsorption of inhibitor on the surface of the mild stee l[17]. The raise in efficiency (IE%) with increase in temperature and invariance of inhibitor efficiency with immersion time beyond 12 h indicates chemisorption.

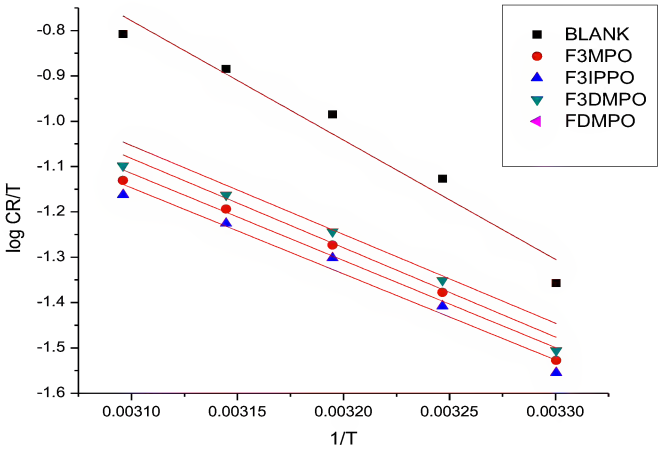

Figure 3: The Transition State Plot of MS Corrosion in 1N H_2SO_4 Solution Containing Inhibitors

The Electrochemical Impedance Spectroscopy

The corrosion behaviour of mild steel in 1N H_2SO_4 and 1N HCl in the presence and absence of the inhibitor compounds has been investigated using EIS at room temperature. Nyquist plots of mild steel in uninhibited and inhibited acid solution containing various concentrations of F3MPO, F3IPPO, F3DMPO and FDMPO are given in Figures 4, 5, 6,7 and 8. As all the inhibitors gave similar spectra only representative plots are given. A single capacitative loop is observed at all concentrations from 0.1 mM to 5 mM and all the impedance spectra have been measured at the respective corrosion potential and analysed in terms of an Randles equivalent circuit with the help of Ivium software. These circuits fall into the classical parallel resistor capacitor combination, the series resistor being that of the solution. In the circuit, R_s represents the solution resistance and R_{ct} the polarization resistance and Q a constant phase element (CPE) whose admittantance is defined as $Q = Y_o (j2\pi f)^n$

The inhibition efficiencies were calculated from the R_{ct} data using the formula given below and are shown in Tables 7 and 8.

$$IE(\%) = \left(\frac{R_{ct(inh)} - R_{ct\ (Blank)}}{R_{ct(inh)}} \right) \times 100 \quad (2)$$

Where $R_{ct(inh)}$ is the charge transfer resistance for inhibited solution and $R_{ct\ (Blank)}$ is the charge transfer resistance for uninhibited solution.

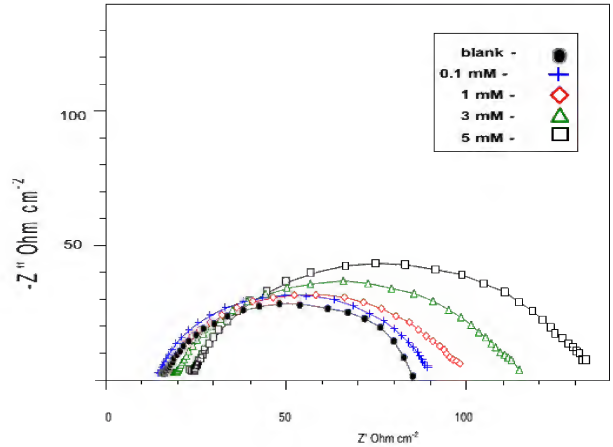

Figure 4: The Nyquist Plots for MS in 1N H_2SO_4 in the Presence and in the Absence of F3MPO

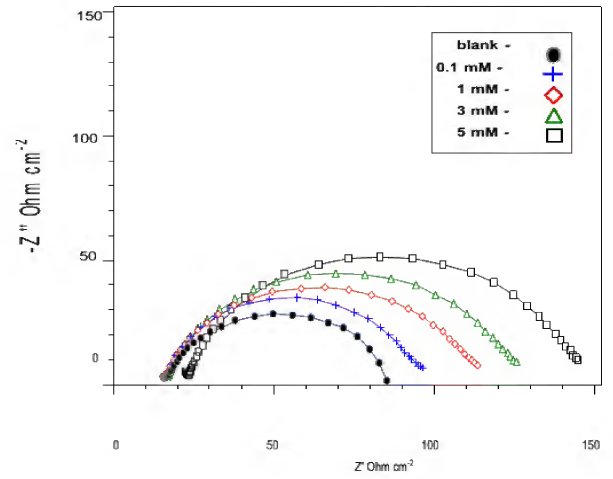

Figure 5: The Nyquist Plots for MS in 1N H_2SO_4 in the Presence and in the Absence of FDMPO

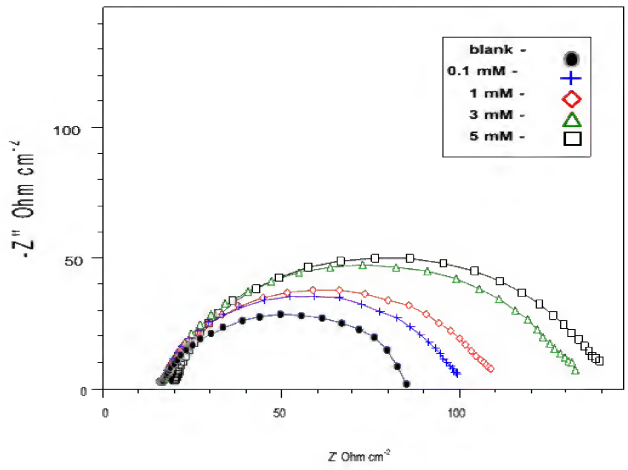

Figure 6: The Nyquist Plots for MS in 1N H_2SO_4 in the Presence and in the Absence of F3DMPO

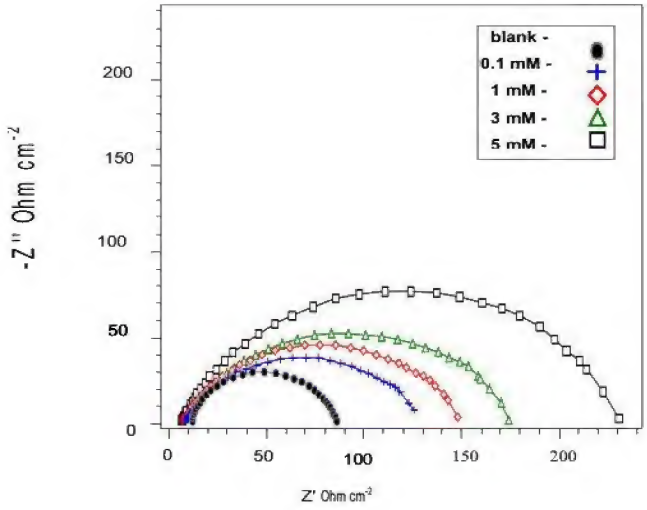

Figure 7: The Nyquist Plots for MS in 1N HCl in the Presence and in the Absence of F3DMPO

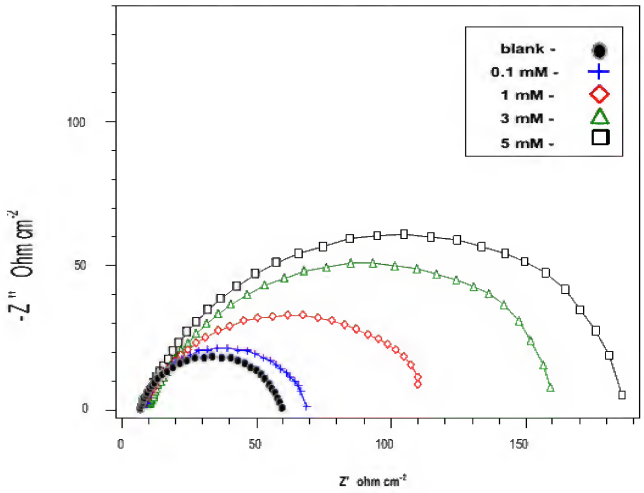

Figure 8: The Nyquist Plots for MS in 1N HCl in the Presence and in the Absence of F3IPPO

The increase in R_{ct} values with an increase in inhibitor concentration is the result of an increase in the surface coverage by the inhibitor molecule which led to increase in inhibitor efficiency. The decrease in the C_{dl} values with the increase in inhibitor concentration is due to the adsorption of the inhibitor molecule replacing water molecule at the metal-solution interface that led to the decrease in local dielectric constant and /or an increase in thickness of the electrical double layer[18]. Hence the change in C_{dl} values which is caused by the gradual displacement of water molecule by the adsorption of the inhibitor at the metal-solution interface decreases the extent of the corrosion[19]. The efficiency of all inhibitors increases with the increase in concentration and shows the same trend as in gravimetric measurements F3IPPO>F3MPO>F3DMPO>FDMPO in both the media.

Potentiostatic Polarization Study

Figures 9, 10,11,12 and 13 show polarization curves of mild steel in 1N H_2SO_4 and 1N HCl in the presence and absence of various concentration of F3MPO, F3IPPO, F3DMPO and FDMPO. It is obvious that the addition of inhibitors hindered the acid attack on the mild steel electrode and increasing the concentration of the inhibitor gave rise to a consistent decrease in anodic and cathodic current densities indicating that F3MPO, F3IPPO, F3DMPO and FDMPO act as a mixed type inhibitors[20].

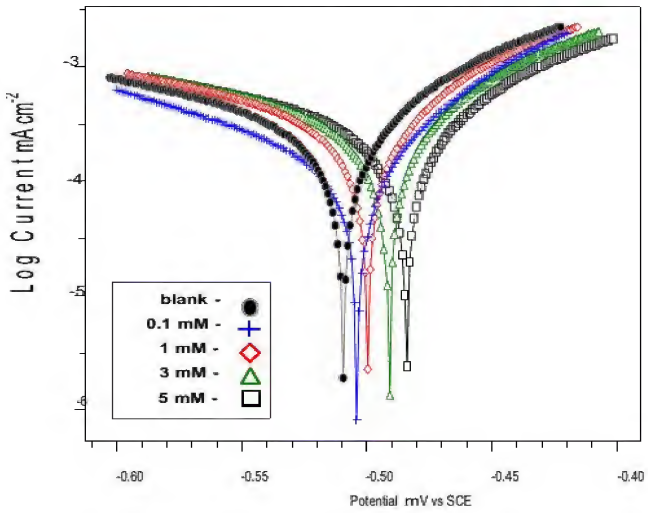

Figure 9: The Tafel Plots for MS in 1N H_2SO_4 in the Presence and in the Absence of F3MPO

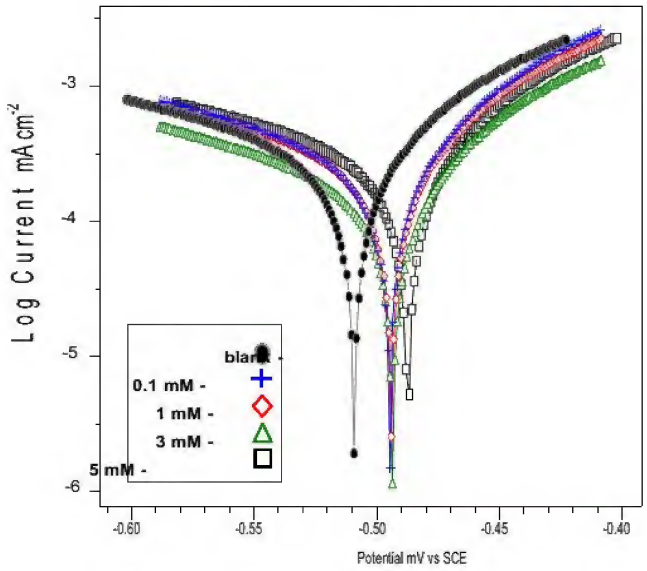

Figure 10: The Tafel Plots for MS in 1N H_2SO_4 in the Presence and in the Absence of FDMPO

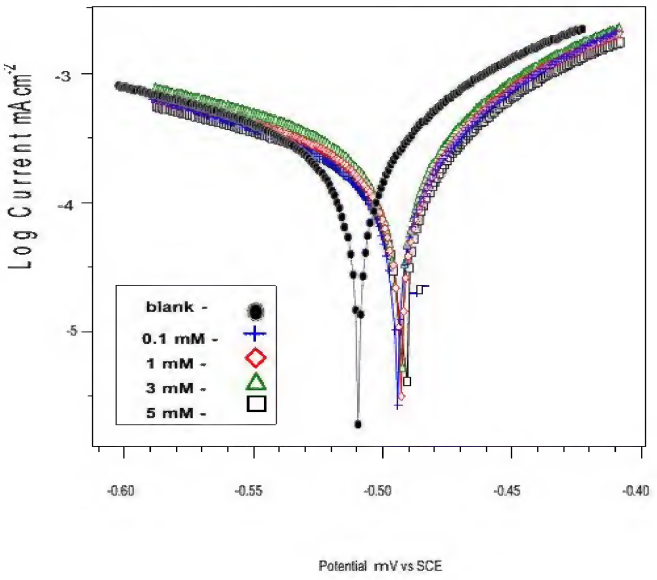

Figure 11: The Tafel Plots for MS in 1N H_2SO_4 in the Presence and in the Absence of F3DMPO

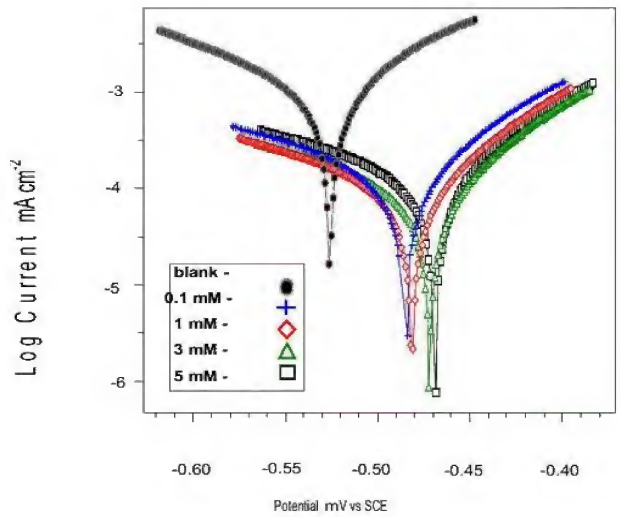

Figure 12: The Tafel Plots for MS in 1N HCl in the Presence and in the Absence of F3DMPO

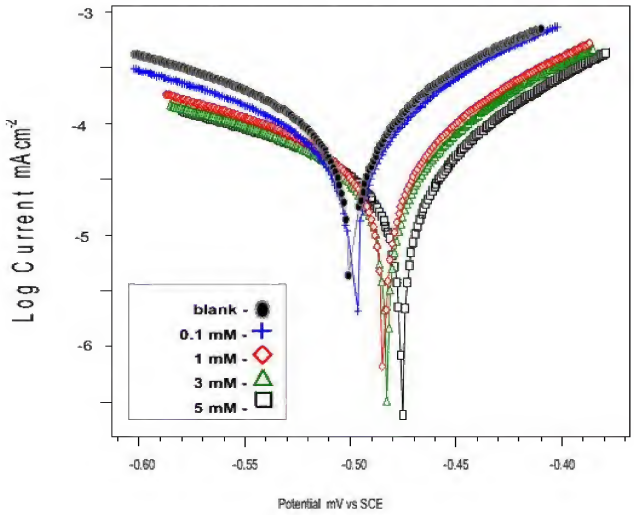

Figure 13: The Tafel Plots for MS in 1N HCl in the Presence and in the Absence of F3IPPO

The corrosion potential (E_{cor}), corrosion current density (I_{cor}), Tafel slope β_a , β_c which are obtained by extrapolation of the Tafel lines are listed in Tables 7 and 8. The calculated percentage inhibition efficiency (IE%) are also given in Tables 7 and 8. Analysis of these data shows that I_{corr} decreased with the addition of inhibitors in 1N H_2SO_4 and 1N HCl due to the increase in the blocked fraction of the electrode surface by adsorption. The E_{corr} value is also shifted towards the more noble side with an increase in the inhibitor concentration.

Adsorption Isotherm

In order to understand the mechanism and nature of adsorption attempts were made to fit surface coverage values θ to various isotherms including Frumkin, Langmuir and Temkin. The best fit was obtained with both the Langmuir and Tempkin Isotherms (Figures 14,15,16 and 17). According to Langmuir isotherm, θ is related to concentration of the inhibitor C_{inh} *via*

$$\frac{\theta}{1-\theta} = kC_{inh} \exp\left(\frac{-\Delta G^{\circ}_{ads}}{RT}\right) \quad (3)$$

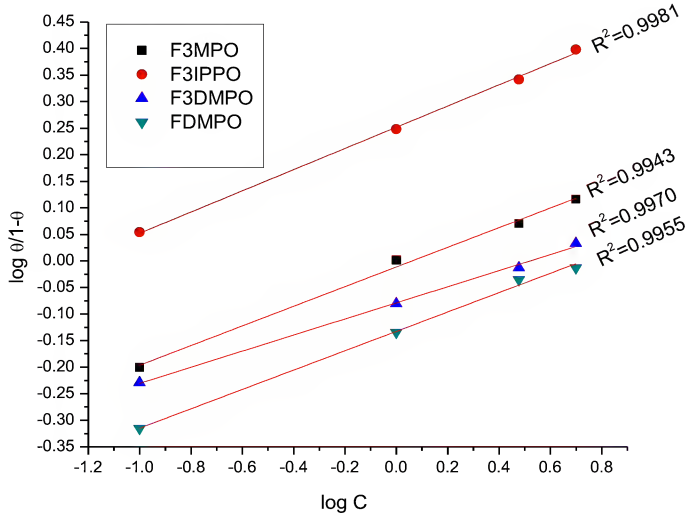

Figure 14: The Langmuir Isotherms for the Adsorption of Inhibitors in 1N H_2SO_4 Solution

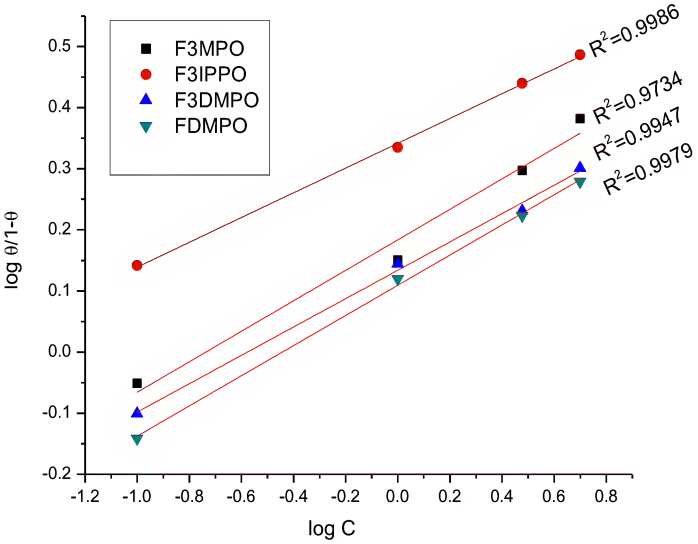

Figure 15: The Langmuir Isotherms for the Adsorption of Inhibitors in 1N HCl Solution

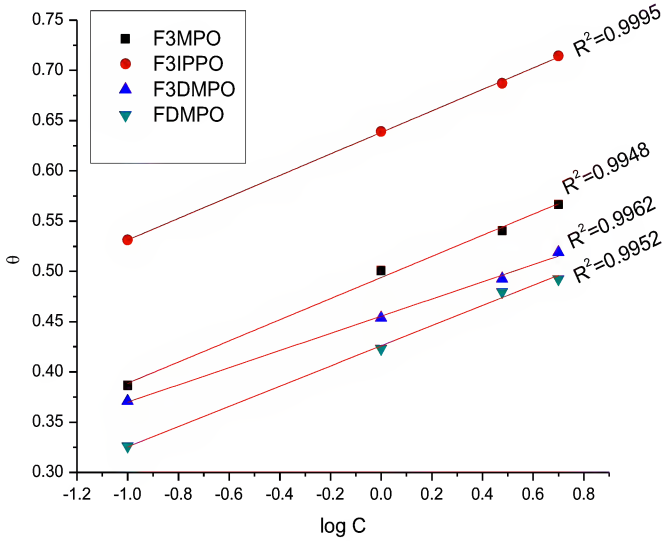

Figure 16: The Tempkin Isotherms for the Adsorption of Inhibitors in 1N H_2SO_4 Solution

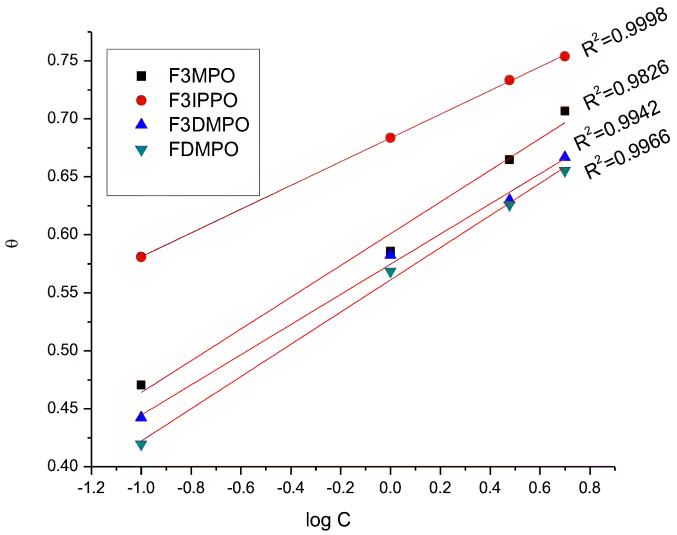

Figure 17: The Tempkin Isotherms for the Adsorption of Inhibitors in 1N HCl Solution

This equation predicts a linear plot between the values of log (θ/1-θ) and log C_{inh}, ΔG°_{ads} is the free energy of adsorption and K is the constant[21]. The strong correlation (r^2 = 0.9911) in 1N HCl and (r^2 = 0.9962) in 1N H_2SO_4 for the Langmuir adsorption isotherm for the inhibitors confirms the validity of this approach. Like many organic inhibitors *N*-formyl piperidin-4-ones also follows Tempkin's Isotherm with a high correlation (r^2 = 0.9933) in 1N HCl and (r^2 = 0.9964) in 1N H_2SO_4.

DISCUSSIONS

As far as the inhibition process is concerned it is generally assumed that adsorption of the inhibitor at the metal-solution interface is the first step in the mechanism of inhibitors in aggressive media. Four types of adsorption may take place involving organic molecules at the metal-solution interface: (1) electrostatic attraction between charged molecules and the charged metal, (2) the interaction of unshared electron pairs in the molecule with the metal, (3) interaction of π electrons with the metal and (4) a combination of the above[22].

Chemisorption involves charge sharing or charge transfer from the inhibitor molecule to the mild steel surface to form a coordinate covalent type bond. The electron transfer is reckoned for transition metals having vacant, low-energy electron orbital. Inhibition efficiency depends on several factors such as the number of adsorption sites and their charge density, molecular size of the inhibitor molecule, mode of interaction with the metal surface and formation of metallic complexes [23].

The *N*-formyl inhibitor interferes in the dissolution reaction by adsorption on metal surface in two different ways. First, the inhibitor competes with Cl^- or SO_4^{2-} ions for anodic sites which are originally water covered. In the process of adsorption, the protonated inhibitor loses its associated proton(s) in entering the double layer and chemisorbs by donating electrons to the metal. In addition, the protonated inhibitor electrostatically adsorbs on to the anion covered surface through its cationic form. *N*-formyl inhibitor thus plays a predominant role by participating in a number of adsorption – desorption steps, rather than by a mere blockage of sites [16, 24, 25].

The binding character of inhibitor on the mild steel surface can be interpreted by means of coordination bonds using electron pairs of oxygen atom and π electrons of the benzene ring. Better corrosion inhibition can be obtained

through the formation of true chemical bonds between organic molecule and metal surface. Hence it can be concluded that inhibition of corrosion of mild steel by *N*-formyl piperidin-4-ones in aggressive medium is due to the adsorption of Fe^{+2} – inhibitor complex, coordinated with electron pairs of oxygen atoms of both the carbonyl groups.

As chloride ions are more strongly adsorbed on the iron surface than sulphate ions, the cationic form of the formyl inhibitor molecule can adsorb on the metal surface with relative ease in HCl compared with H_2SO_4 [18, 20] thus accounting the high inhibitor efficiency in HCl medium than in H_2SO_4.

As the process of inhibition occurs through the phenomenon of adsorption, it is necessary to develop suitable mechanism for the adsorption of *N*-formyl piperidin-4-ones on the carbon steel surface. Damaskin *et al.*[26] suggested that the adsorption of organic molecule on different type of metallic surfaces occurs through competitive adsorption between organic compound and water molecules. The higher free energy of adsorption for organic compounds than for water molecule facilitates such adsorption. Sankarapapavinasam *et al.*[12] have analysed the adsorption of piperidine and few piperidones *viz.* 2,6-diphenylpiperidin-4-one, 3-methyl-2,6-diphenylpiperidin-4-one, 2,2-dimethyl-2,6-diphenylpiperidin-4-one on the corrosion of copper and sulphuric acid. They have proposed that the interaction of piperidone with the metal surface could occur through >C=O or –NH group. The lower electronegativity of the nitrogen atom favours NH as an anchoring site with chair conformation, but involvement of both groups was ruled out by them as it would need the piperidones to be in strained boat conformation. Muralidharan et al.[20] and Mallika et al.[27] have also concluded that piperidones adsorb through nitrogen lone pair in chair conformation.

However, Ravichandran *et al.*[28] have proposed that the piperidin-4-ones adsorbed through both - NH and >C=O groups at positions 1 and 4, respectively, with strained boat conformation using IR spectral studies. The carbonyl adsorption peak around 1700 cm^{-1} has disappeared completely when N-H stretching band around 3000-3500 cm^{-1} and C-N stretching around 1000-1350 cm^{-1} have been altered. A new O-H stretching band at 3000-3500 cm^{-1} has appeared. They also proposed that after adsorption on mild steel surface, the carbonyl group is reduced catalytically to C-OH group to axial alcohol to facilitate the continued adsorption in the boat form.

Jeyaraman *et al.* [3] have shown that the preferred conformation of *N*-formyl-*cis*-2,6-diaryl piperidin-4-ones in solution were found to be flattened boat with the aryl groups in quasi-axial position which is shown in Figure 18. The severe $A^{1,3}$ strain due the interaction between –N-C=O group (coplanar to C2-N1-C6 plane) and the adjacent phenyl groups forces the *N*-formyl-*cis*-2,6-diarylpiperidin-4-ones to prefer flattened boat conformation. They also averred that a hydrogen bond type of attraction between the electron rich oxygen atom of –N-C=O group and the electron deficient hydrogen at α-position stabilises the flattened boat conformation

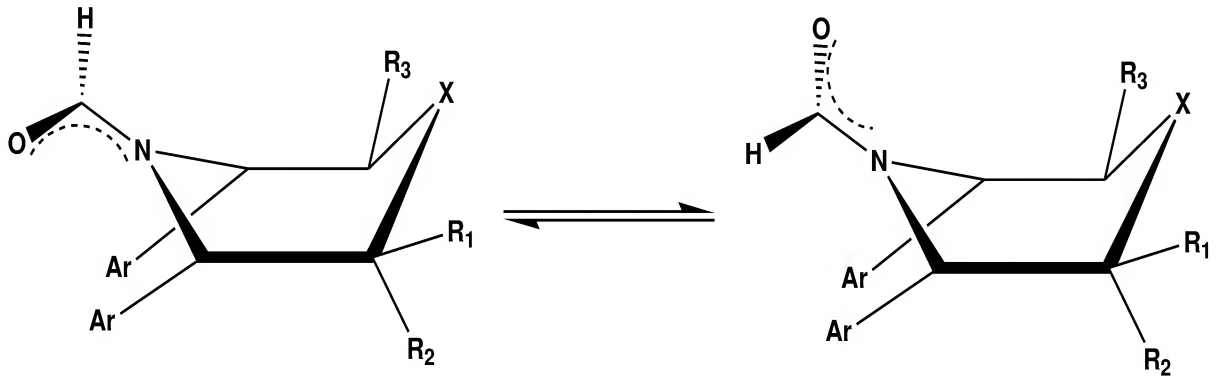

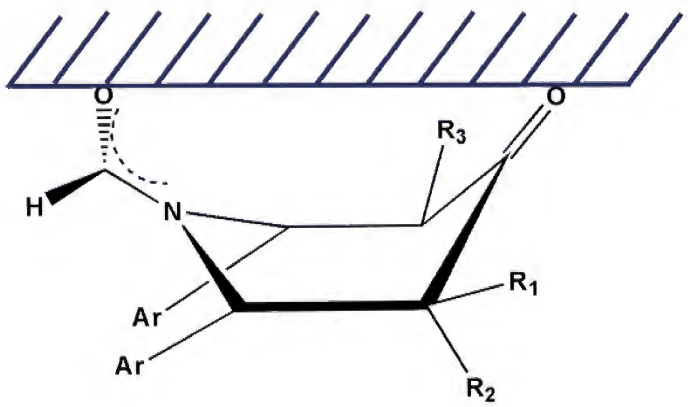

Figure 18: Mode of Adsorption of *N*-Formylpiperidin-4-Ones in the Flattened Boat Conformation

The FT-IR spectra of F3MPO, F3IPPO, F3DMPO and FDMPO are recorded using Perkin-Elmer 1600 FT-IR spectrometer and are shown in Figures 19 (a) to 22 (a), respectively. FT-IR spectra of the adsorbed material scratched from the metal surface is shown in Figures 19 (b) to 22 (b). On careful observation of FT-IR spectra it is evident that the carbonyl frequency of the amide group appeared around 1660 cm^{-1} and the carbonyl frequency of the ring group appeared at 1710 cm^{-1} were absent and shifted down to 1503 cm^{-1} - 1530 cm^{-1}. These shifts in >C=O stretching can be attributed to the shift of electron density of the >C=O towards Fe^{+2} resulting in the formation of Fe^{+2} – inhibitor complex thus controlling the corrosion. Moreover the carbonyl group gets reduced to alcohol and continues to be adsorbed on the MS surface whose stretching frequency shifted higher to 3500 cm^{-1} - 3700 cm^{-1} in the product molecule. The mechanism of inhibition is portrayed in Figure 18.

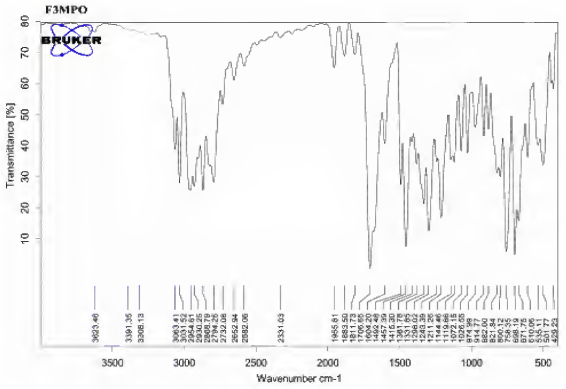

Figure 19: (a) F3MPO

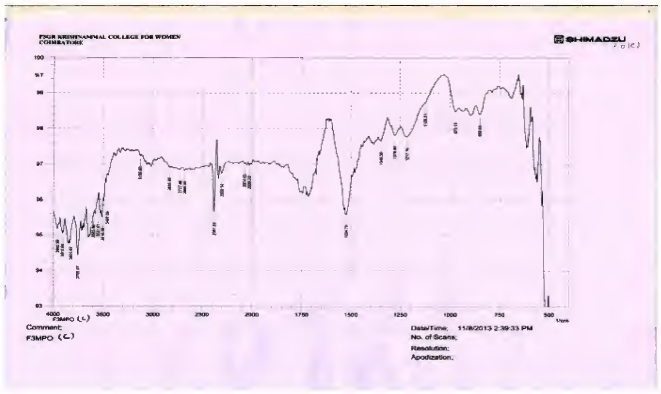

Figure 19: (b) F3MPO (Compound)

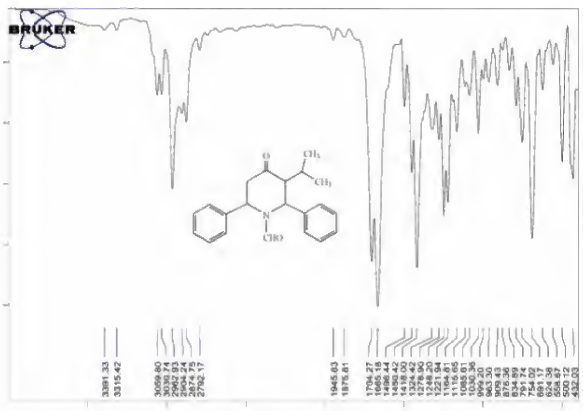

Figure 20: (a) F3IPPO

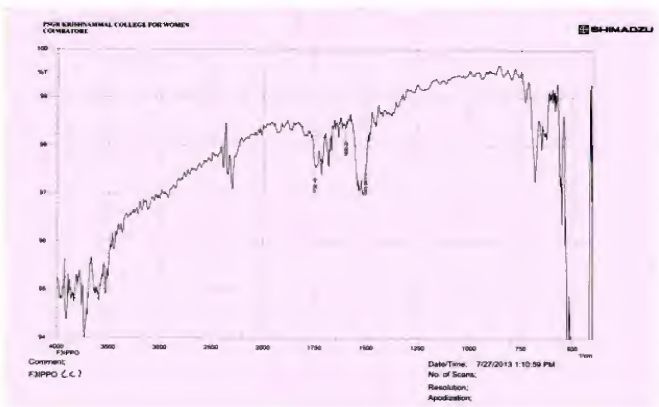

Figure 20: (b) F3IPPO (Compound)

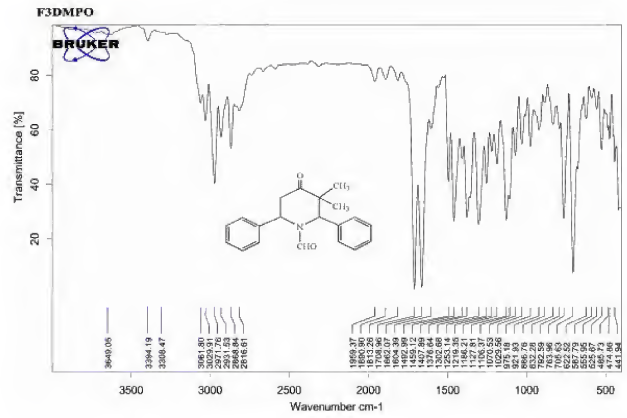

Figure 21: (a) F3DMPO

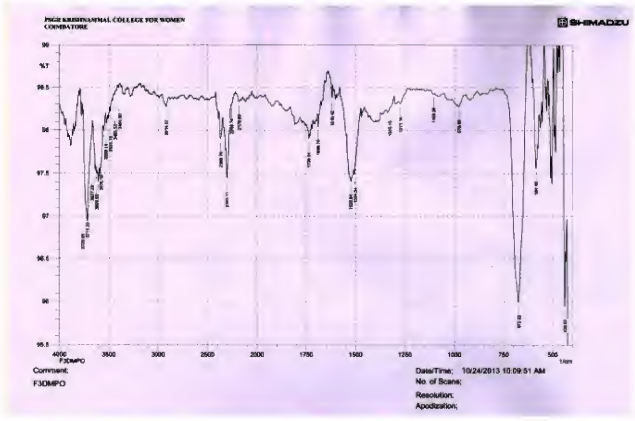

Figure 21: (b) F3DMPO (Compound)

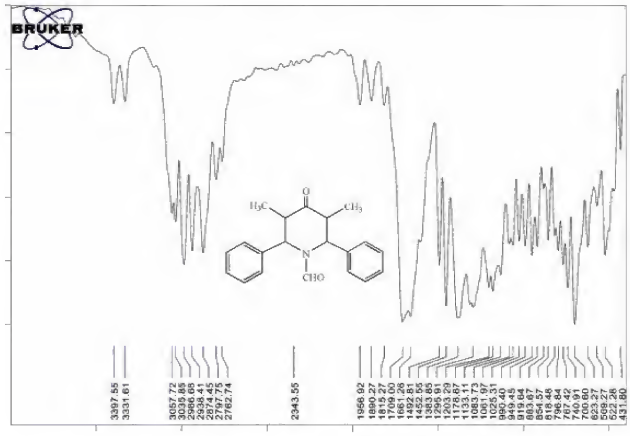

Figure 22: (a) FDMPO

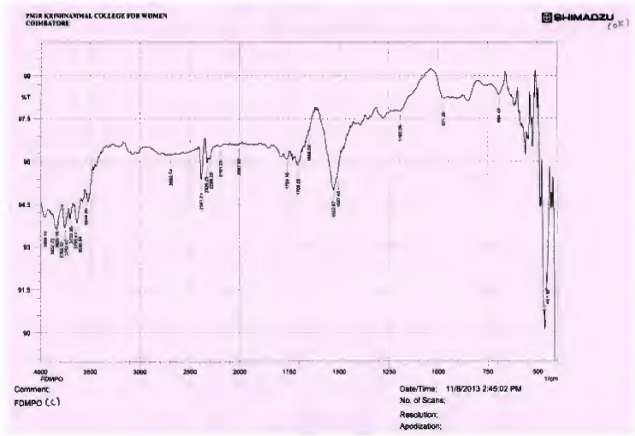

Figure 22: (b) FDMPO (Compound)

Surface Analysis

The surface morphology was studied by SEM and EDS and given in Figures 23(a), 23(b), 23(c), and 23(d). The uninhibited SEM picture [23(a)] shows the distribution of corrosion products on the surface and the inhibited SEM picture [23(b)] vividly shows the presence of adsorbed inhibitor molecule on the surface thus preventing corrosion.

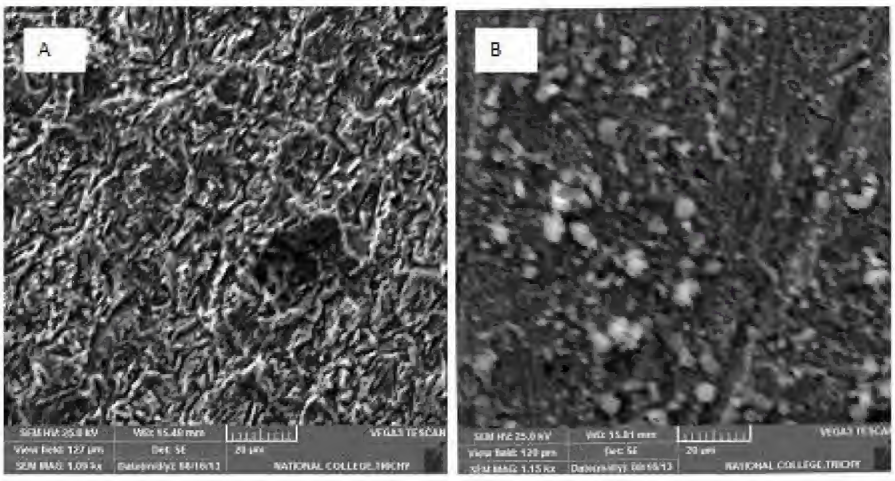

Figures 23: Show the SEM Image of Uninhibited MS Surface (A) MS Surface Inhibited by FDMPO (B)

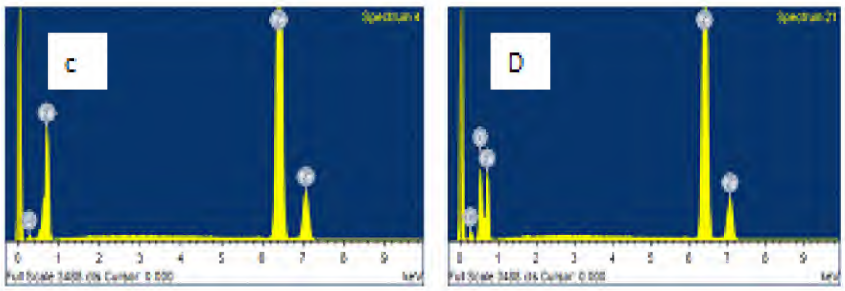

Figure 24

Element	Weight %	Atomic%
C	9.32	23.49
O	20.24	38.31
Fe	70.45	38.20
Total	100	

Element	Weight %	Atomic%
C	6.51	24.46
Fe	93.49	75.54
Total	100	

CONCLUSIONS

All the *N*-formyl derivatives of piperidine-4-ones show good inhibition efficiency in both 1N H_2SO_4 and 1N HCl medium. The inhibition efficiency of the *N*-formyl piperidin-4-ones follows the order: F3IPPO > F3MPO > F3DMPO > FDMPO. The protection efficiency increases with the increase in concentration and reaches a maximum of 5 mM concentration. The polarization studies show that the inhibitors suppress both anodic and cathodic corrosion and thus act as mixed inhibitors. The single loop in the electrochemical impedance spectroscopy shows that the inhibition is by adsorption of the inhibitor on the mild steel surface and blocking the active sites. FT-IR spectra show that the adsorbed material consists of Fe^{+2} – inhibitor complex. The adsorption of inhibitor correlates well with both Langmuir and Tempkin adsorption Isotherms. The inhibition efficiency increases with the increase in temperature up to 323K and immersion time 12 h.

REFERENCES

1. G. Trabanelli, *Corrosion* **47** (1991) 410.
2. T. Ravindran, R. Jeyaraman, R. W. Murray and M. Singh, M. *J. Org. Chem.* **56** (1991) 4833.
3. R. Jeyaraman, J. C. Thenmozhiyal, R. Murugadoss and M. Venkatraj,. *Indian J. Chem.* **38B** (1999) 325.
4. P. Sakthivel, Ph.D. Thesis, Bharathiar University, India (2014).
5. C. R. Noller and V. Baliah, V. *J. Am. Chem. Soc.,* 70 (1948) 3853.
6. S. Ponnuswamy, R. Murugadoss, R. Jeyaraman, A. Thiruvalluvar and V. parthasarathy *Indian J. Chem.* **45B** (2006) 2059.
7. K. Ravichandran, P. Sakthivel, P. Ramesh, S. Ponnuswamy and M. N. Ponnuswamy *Acta Cryst.* **E68** (2012) 0870.

8. K. Ravichandran, P. Ramesh, P. Sakthivel, S. Ponnuswamy and M. N. Ponnuswamy *Acta Cryst.* **E66** (2010) 1505.
9. T. kavitha, P. Sakthivel, S. Ponnuswamy, S. S. Ilango and M. N. Ponnuswamy *Acta Cryst.* **E65** (2009) 2818.
10. S. Ponnuswamy, M. Venkatraj, R. Jeyaraman, M. Sureshkumar, D. Kumaran, D and M. N. Ponnuswamy *Indian J. Chem.* **41B** (2002) 614.
11. F. Bentiss, M.Traisnel, M.Lagrenee, *Corros. Sci.* **42** (2009) 127.
12. Sankarapapavinasam, F. Pushpanathan and M. F. Ahmed, *Corros. Sci..,* **32** (1989) 193.
13. R.S. Chaudhary, S. Ind. Sharma, *J.Chem. Technol.* **6** (1999) 202.
14. S.A. Umoren, I.B. Obot, E.E. Ebenso and N.O. obi-Egbedi, *Desalination*. **250** (2009) 225
15. N. Hackermann, E.S. Snavel and J.S. Payne, *J. Electrochem. Soc.,* **113** (1966) 677.
16. N. Hackermann and E. McCafferty, *Proceedings of the 5th international Congress on "Metalic Corrosion"* (Tokyo, 1972), p. 542
17. H. B. Rudresh and S.M. Mayanna, *J. Electrochem. Soc. India,* **31** (1982) 109.
18. M. Behpour, S.M. Ghoreshi, A. Gandomi-Niasar, N. Soltani and M. Salavati-Niasari, *J. Mater. Sci.* **44** (2009) 2444.
19. M. Benabdellah, R. Touzani, A. Aouniti. A. Dafali, S. El Kadiri, B. Hammoutia and M. Benkadddour, *Mater. Chem. Phys.* **105** (2007) 373.
20. S. Muralidharan, K.L.N. Phani, S. Pitchumani, S. Ravichhandran and S.V.K. Iyer, *J. Electrochem. Soc.* **142** (1995) 1478.
21. S. Kertit and B. Hammouti, *Appl. Surf. Sci.* **93** (1996) 59.
22. F. Bentiss, M. Traisnel, M. Lagrenee, *J. Applied Electrochem.* **31** (2001) 41.
23. A. Fouda, M. Moussa, F. Taha and El Neanaa, *Corros. Sci.* **26** (1986) 719.
24. N. Hackermann, E.S. Snavel, Jr and J.S. Payne, Jr, *J. Electrochem. Soc.* **113** (1966) 677.
25. T. Murakawa and N. Hackermann, *Corros. Sci.* **4** (1964) 387.
26. Boris B. Damaskin, Oleg A. Petrii and Valerii. V. Batrakov, "*Adsorption of Organic Compounds on Electrodes*", Plenum Press, New York, London, (1971) 262 – 266.
27. J. Mallika, Ph.D. Thesis, Bharathiyar University, India (2002).
28. J. Ravichandran, Ph.D. Thesis, Bharathiyar University, India (2006).

APPENDICES

Table 1: Inhibiting Efficiency from Weight Loss Measurements

Inhibitor+40 ml Ethyl Alcohol.	Concentration (mM)	H_2SO_4			HCl		
		Weight Loss (mg)	Corrosion Rate (mm /y)	IE%	Weight Loss (mg)	Corrosion Rate (mm /y)	IE%
F3MPO	Blank: + 40 ml ethyl alcohol	7.715	11.436		10.95	16.232	
	0.1	4.733	7.0162	38.65	5.791	8.5846	47.05
	1.0	3.852	5.7102	50.07	4.535	6.7227	58.58
	3.0	3.546	5.2566	54.04	3.671	5.4419	66.48
	5.0	3.343	4.9557	56.66	3.211	4.7600	70.68
F3IPPO	0.1	3.617	5.3618	53.12	4.589	6.8027	58.09
	1.0	2.784	4.1270	63.91	3.463	5.1336	68.37
	3.0	2.413	3.5770	68.72	2.918	4.3256	73.35
	5.0	2.204	3.2672	71.43	2.694	3.9936	75.4
F3DMPO	0.1	4.852	7.1926	37.11	6.107	9.0530	44.23
	1.0	4.213	6.2454	45.39	4.473	6.6308	58.24
	3.0	3.914	5.8021	49.27	4.051	6.0052	63
	5.0	3.712	5.5027	51.91	3.647	5.4063	66.69
FDMPO	0.1	5.200	7.7085	32.6	6.358	9.4251	41.94
	1.0	4.453	6.6011	42.32	4.724	7.0029	56.86
	3.0	4.014	5.9504	47.97	4.098	6.0749	62.58
	5.0	3.915	5.8036	49.25	3.774	5.5946	65.53

Table 2: Effect of Immersion Period on the 1mM Inhibitors of the Corrosion of MS in H_2SO_4 Media

Immersion Period in h	Blank CR (mm/y)	F3MPO		F3IPPO		F3DMPO		FDMPO	
		CR (mm/y)	IE(%)	CR (mm/y)	IE(%)	CR (mm/y)	IE(%)	CR (mm/y)	IE(%)
1	9.051	6.419	29.080	5.606	38.062	7.770	14.153	7.924	12.452
3	17.184	10.102	41.213	8.991	47.678	11.516	32.984	11.977	30.301
6	32.38	15.626	51.742	14.070	56.547	17.137	47.075	18.058	44.231
9	47.582	21.150	55.550	19.148	59.758	22.757	52.173	24.139	49.269
12	62.782	26.674	57.513	24.226	61.413	28.377	54.801	30.220	51.865
24	123.579	50.769	58.918	46.538	62.341	54.859	55.608	58.543	52.627

Table 3: Effect of Addition of 1mM Anions on the Corrosion Inhibition of MS in 1N H_2SO_4

System	(1mMF3MPO)			(1mM F3IPPO)			(1mM F3DMPO)			(1mM FDMPO)		
	Weight Loss (mg)	Corrosion Rate (mm/y)	IE (%)	Weight Loss (mg)	Corrosion Rate (mm/y)	IE (%)	Weight Loss (mg)	Corrosion Rate (mm/y)	IE (%)	Weight Loss (mg)	Corrosion Rate (mm/y)	IE (%)
Blank	4.833	7.164		4.492	6.658		5.33	7.9		5.66	8.39	
KNO_3	4.166	6.176	13.80	4.147	6.148	7.68	4.29	6.359	11.51	5.00	7.412	11.65
KCNS	4.00	5.92	17.23	3.942	5.844	12.24	4.46	6.612	16.32	4.92	7.293	13.18
KCl	3.66	5.434	24.14	3.82	5.663	14.96	4.38	6.49	17.82	4.66	6.908	17.668
$KBrO_3$	3.166	4.694	34.47	3.41	5.055	24.08	3.56	5.277	33.21	3.9	5.781	31.09
KBr	2.833	4.199	41.37	3.00	4.447	33.21	2.89	4.284	45.78	3.83	5.677	32.33
KI	1.833	2.717	62.07	1.923	2.853	57.19	2.39	3.543	55.16	3.00	4.447	46.998

Table 4: Effect of the Temperature and Corrosion Inhibition of MS in H_2SO_4 Medium

System	303K		308K		313K		318K		323K	
	CR (mm/y)	IE (%)	CR (mm/y)	IE (%)	CR (mm/y)	IE (%)	CR (mm/y)	IE (%)	CR (mm/y)	IE (%)
Blank	13.319	-	23.00	-	32.367	-	41.423	-	50.245	-
F3MPO	8.993	32.48	12.904	43.90	16.694	48.42	20.362	50.84	23.919	52.40
F3IPPO	8.455	36.59	12.048	47.62	15.639	51.68	18.927	54.307	22.241	55.73
F3DMPO	9.455	29.02	13.728	40.31	17.875	44.78	21.869	47.205	25.754	48.74
FDMPO	10.149	23.80	14.697	36.10	19.121	40.92	23.367	43.589	27.502	45.26

Table 5: Thermodynamic Parameter

Inhibitor	E_a (KJmol^{-1})	$\Delta H^{\#}$(KJmol^{-1})	$\Delta S^{\#}$(JK^{-1}mol^{-1})
BLANK	52.995	50.394	-56.251
F3MPO	39.379	36.778	-104.91
F3IPPO	38.948	36.347	-106.851
F3DMPO	40.318	37.717	-101.361
FDMPO	40.115	37.515	-101.446

Table 6: ΔG^{O} (KJmol^{-1})

Inhibitor	303K	308K	313K	318K	323K
F3MPO	-8.276	-9.658	-10.289	-10.709	-11.045
F3IPPO	-8.734	-9.880	-10.629	-11.078	-11.406
F3DMPO	-7.866	-9.130	-9.908	-10.325	-10.652
FDMPO	-7.188	-8.681	-9.498	-9.939	-10.277

Table 7: Electrochemical Parameters for MS Corrosion in 1 N H_2SO_4 + 40 ml Ethyl Alcohol with Different Concentrations of the Inhibitor

	Conc. of Inhibitor (mM)	R_{ct} Ohm cm^2	C_{dl} (F) *10^{-5}	IE (%)	β_a (mV)	β_c (mV)	I_{corr} (µA/CM^2)	-E_{corr} (mV)	Corrosion Rate (mm/y)	R_p Ohm	IE (%)
	BLANK	29.39	3.09		78	145	373.8	511.1	5.596	102.3	
F3MPO	0.1	60.0	3.37	51.02	80	163	241.8	504.1	6.1	94.39	35.31
	1	66.6	3.31	55.87	79	153	203.2	499.9	5.995	99.29	45.63
	3	87.3	3.09	66.36	76	156	168.0	491.5	5.64	107.9	55.06
	5	94.0	2.66	68.73	62	126	151.7	484.0	4.1	152	59.42
F3IPPO	0.1	64.2	3.51	54.22	78	156	232.6	507.6	5.56	104.2	37.77
	1	73.4	3.42	59.96	74	152	201.3	498.6	4.72	121.6	46.15
	3	91.6	3.02	67.91	73	140	162.1	494.3	3.89	143.2	56.63
	5	104.6	2.56	71.90	63	133	120.2	490.2	3.72	162.3	67.84
F3DMPO	0.1	56.8	2.75	48.25	76	154	253.6	503.2	5.58	106.2	32.16
	1	68.6	2.91	57.15	73	153	205.6	498.1	4.61	129.2	44.50
	3	80.3	2.69	63.40	72	152	173.2	493.2	3.989	152.6	53.67
	5	90.2	2.64	67.41	67	130	165.2	490.4	3.85	161.4	55.81
FDMPO	0.1	54.8	3.89	46.37	76	154	273.3	495.8	3.85	102.8	26.89
	1	66.6	2.98	55.87	72	153	225.6	495.1	3.989	120.8	39.65
	3	81.4	2.89	63.89	67	153	195.2	494.1	4.61	133.0	47.78
	5	87.8	2.50	66.53	73	130	188.4	494.6	5.586	141.1	49.59

Table 8: Electrochemical Parameters for MS Corrosion in 1N HCl + 40 ml Ethyl Alcohol with Different Concentrations of the Inhibitor

	Conc. of Inhibitor (mM)	R_{ct} Ohm cm^2	C_{dl} (F) *10^{-5}	IE (%)	β_a (mV)	β_c (mV)	I_{corr} (µA/CM^2)	-E_{corr} (mV)	Corrosion Rate (mm/y)	R_p Ohm	IE (%)
	BLANK	34.3	7.34		81	133	313.7	496.8	1.026	89.43	
F3MPO	0.1	60.1	7.78	42.93	81	140	200.6	496.6	0.7992	114.9	36.05
	1	87.2	5.37	60.67	78	139	144.0	484.3	0.504	180.6	45.41
	3	108.3	4.38	68.33	75	137	122.6	482.7	0.4154	213.4	60.92
	5	133.5	4.09	74.31	74	136	107.6	475.9	0.3522	248.4	65.70
F3IPPO	0.1	82.6	5.73	58.47	69	142	124.6	482.8	1.894	203.2	60.28
	1	100.8	5.24	65.97	66	133	101.8	479.3	1.851	211.4	67.55
	3	117.8	5.43	70.88	65	135	90.5	470.0	1.375	269.7	71.15
	5	172.1	4.51	80.07	69	135	83.8	467.2	1.274	289.6	73.29
F3DMPO	0.1	62.4	5.73	45.03	78	141	144.6	492.4	1.984	140.0	53.91
	1	90.3	5.24	62.02	74	137	132.8	486.4	1.582	186.3	57.64
	3	102.6	5.43	66.05	75	136	127.0	479.2	1.423	254.3	59.52
	5	125.4	4.51	72.64	72	132	110.0	472.1	1.123	282.6	64.93
FDMPO	0.1	58.6	6.32	41.47	79	141	164.2	493.2	1.752	120.2	47.66
	1	87.2	5.37	60.67	78	133	154.6	488.4	1.651	160.3	50.72
	3	98.6	4.22	65.21	74	138	132.2	482.3	1.212	220.6	57.86
	5	120.2	3.89	71.46	75	136	116.0	478.6	1.134	260.4	63.02